REPORT

CAVITY COOLING OF A LEVITATED NANOSPHERE BY COHERENT SCATTERING

UROŠ DELIĆ, MSC*

FACULTY OF PHYSICS, UNIVERSITY OF VIENNA

Supervisor at the University of Vienna:
Prof. Dr. Markus Aspelmeyer

Supervisor at the host institution (Massachusetts Institute of Technology):
Prof. Dr. Vladan Vuletić
The work presented below has been conducted during a three month research visit to the Massachusetts Institute of Technology (MIT).

1 INTRODUCTION

Field of cavity optomechanics has already enjoyed a lot of success with different mechanical oscillators [1]. Optically levitated nanospheres were proposed as a new optomechanical system in several papers for their promise of unprecedented mechanical quality factors and strong interaction with light [2, 3, 4], which is based on the absence of mechanical suspension and achievable better isolation from the environment. A good measure of reaching a regime of strong interaction is optomechanical cooperativity C:

$$C = \frac{4g^2}{\kappa\Gamma}, \tag{1}$$

where g is coupling of mechanical motion to light, κ is decoherence due to photon loss from the cavity and Γ is decoherence by heating of oscillator's motion. The partial decoupling from thermal environment promises a large force sensitivity [5] and leads to an experimental regime of room-temperature quantum optomechanics. Realizing a quantum superposition of a nanosphere [6] or teleportation of quantum state of light to a nanosphere [7] is an achievable goal with this system, given large enough optomechanical cooperativity.

Although mechanical damping through collisions with remaining gas is suppressed, at extremely low pressures ($\sim 10^{-7}$ mbar) recoil heating by lasers would rise as dominant source of decoherence. In a regime where nanosphere radius r is smaller than laser wavelength $r \ll \lambda$, nanosphere behaves like a dipole, with dipoles significantly scattering light orthogonally

* *uros.delic@univie.ac.at*

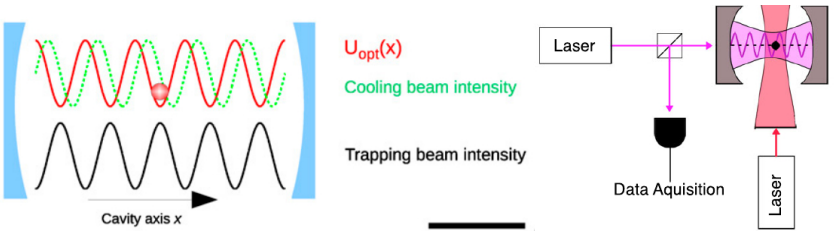

Figure 1: Schemes of the experiment with levitated nanoparticles from [3] (left) and [2] (right). Both proposals include an optical cavity to reach significant cooling and to realize quantum protocols. Experiment on the left has been set up and used in [8]. Experimental setup on the right is currently in operation at the home university.

to the light propagation as well. This leads to additional decoherence compared to other mechanical systems, but can be rendered negligible or even used in experiments. Both atoms and nanospheres behave the same, so in principle we can think of the nanosphere as a large atom. What also speaks in that favor is that nanosphere is a solid body made of SiO_2 molecules with all of the molecules moving in phase due to rigidity. Therefore, atoms and nanospheres should share a similar theoretical approach of coherent scattering. A compilation of important experimental values for both atoms and nanospheres is presented in Section 3.

2 RESEARCH AGENDA

This is to serve as a comparison between proposed research agenda and achieved goals during the research visit.

1. **March 2018:**
   - Literature overview of the work done by the group at the host university.✓
   - Presentation of my research: state of research at the University of Vienna, connection between respective fields and experiments, research goals. ✓
   - Discussion with group members: sharing insights, expectations, literature.✓
   - Work on theory of coherent scattering with a levitated nanosphere in an optical cavity✓

   Outcome: Full theoretical model and study of future experiment at the University of Vienna. Defined best experimental approach and methods that need to be mastered during the research stay.
   Achieved: Full theoretical model has been developed with a help from Prof. Vuletić and is presented in Section 5.

2. **April 2018:**
   - Joining the experiment on cavity cooling of Cs atoms. ✓
   - Learning and sharing techniques on cavities, cavity cooling, noises in experiment, heating mechanisms. ✓

   Outcome: Mastering experimental methods defined in March 2018. Writing experimental protocols.
   Achieved: Through discussion with team members working on the experiment mentioned above, I have gained a valuable insight into various experimental techniques, details and new developments in the field. Summary is presented in Section 7.

3. **May 2018:**
   - Continuing the experimental work. Discussion on further development of the experiment at the host university.✓
   - Final presentation of the research: topics and goals covered, discussing further work at the University of Vienna.

   Outcome: Fully defined research plan for following months at the University of Vienna. Collecting ideas for further projects. Compilation of experimental modifications and measurements to be done at the University of Vienna.
   Achieved: Upon my return to the University of Vienna, plan of experiments and experimental setups has been presented and thoroughly discussed. I gave a talk at our weekly group meeting and presented research perspectives and plans.

3 COMPARISON BETWEEN AN ATOM AND A NANOSPHERE

As we mentioned in introduction, nanosphere interacts with light similarly to an atom, i.e. as a dipole. In order to draw some parallels between a single Cesium atom and a single silica nanosphere used in our experiments ($\rho = 1850\frac{kg}{m^3}$, $r = 71.5$ nm), we developed a summary of important comparisons.

- Mass of a single nanosphere is $m = 2.8 \times 10^{-18}$ kg, while a cesium atom has a mass $m_{Ce} = 2.2 \times 10^{-25}$ kg, seven orders of magnitude smaller. An important implication is that a kick by an atom of any gas present in the vacuum chamber won't severely disturb nanosphere motion due to a large mass difference. Therefore, we don't need to achieve extremely low pressures in comparison to experiments in atomic physics.

- Trapping potential for a polarizable particle depends on polarizability and laser intensity I_0:

$$U = -\frac{\alpha}{2}\frac{2I_0}{\varepsilon_0 c}. \tag{2}$$

  Polarizability of a nanosphere with volume V is given by:

$$\alpha = 3\varepsilon_0 V \frac{n^2(\omega) - 1}{n^2(\omega) + 2} \tag{3}$$

  and has a weak dependency on laser frequency through index of refraction $n(\omega)$. In contrast to nanosphere, atom polarizability depends highly on laser detuning away from atom transition, while it changes a sign at the resonance. Hence, atoms are usually trapped only with lasers being red detuned from atom transition. Nanosphere polarizability is about $h \times 0.5\frac{MHz}{(V/cm)^2}$, while Rydberg atoms can exhibit a similar polarizability once the electron is highly excited. A single cesium atom has a polarizability of only $\sim h \times 0.1\frac{Hz}{(V/cm)^2}$.

- Trap frequencies ω_m are proportional to α/m, which in the case of nanospheres simplifies to $\sqrt{1/\rho}$, e.g. it is independent on neither nanosphere radius nor volume. Trap frequencies for nanosphere and atoms are comparable for comparable laser intensities.

- Given its large mass, amplitude of nanosphere center-of-mass (COM) motion is small even at room temperature ($T = 300$ K) with variance

$\sqrt{\langle x^2 \rangle} \sim 40$ nm. Therefore, they are extremely well confined within trap potential, as standing wave periodicity is $\lambda/2 = 532$ nm. When cesium atoms are trapped in a magneto-optical trap (MOT), temperature of COM motion is $T \sim 200\mu K$, which corresponds to motion on the order of 100 nm.

- Given nanosphere's small amplitude of motion, it is exceptionally easy to reach Lamb-Dicke regime, given by condition $k\sqrt{\langle x^2 \rangle} \ll 1$. In essence, this is equivalent to experiencing low recoil energy $E_{rec}/h = 40$ mHz, transferred to nanosphere motion by a kick of a random photon. It's negligible in comparison to a single phonon of energy $\hbar\omega_m$ (defined by trap frequency ω_m). Hence, a kick by one photon won't be enough to change phonon occupation of nanosphere motion. However, an ensemble of photons from trap laser can at some point give kicks in the same direction, resulting in fast heating (decoherence) of nanosphere motion.

- Trap depth for nanospheres in temperature is typically around 10000 K, which leads to a stable trapping of nanosphere at room temperature. On the other side, atom trap depths are just a bit greater than their motional temperature (~ 1 mK). Trap lifetime of a nanosphere is practically infinite at high pressures. At low pressures (below $\sim 10^{-4}$ mbar), trap nonlinearities can lead to heating of nanosphere motion and subsequent expulsion from the trap.

- Large polarizability also means that we have large scattering rate, typically on the order of $10^{14} \frac{\text{photons}}{\text{s}}$. It's an interplay between this parameter and recoil energy that can lead to significant heating of nanosphere motion. Scattering cross section is about $\sigma_0 \approx 10^{-15} m^2$, roughly of the size of nanosphere cross section.

- Nanospheres can stick to cavity mirrors due to strong, attractive Casimir-Polder force. In comparison to atoms, they pose a real danger to cavity finesse. A couple of nanospheres located around the same point on any mirror can significantly change surface roughness and enhance cavity loss rate.

4 STATE OF RESEARCH

4.1 Current research at the home university

Through strong light-nanosphere coupling, cavity cooling of levitated nanospheres has been demonstrated in multiple experiments in recent years, including our proof-of-concept paper by Kiesel et al. in 2013 [8, 9, 10] and with freely propagating particles in high vacuum (10^{-8} mbar) [11]. However, regime of high cooperativity $C > 1$ is yet to be reached, leading to ground state cooling of nanosphere center-of-mass motion and full quantum control of nanosphere motion. A common obstacle in many experiments is stable levitation of nanospheres at high vacuum, which has so far been shown in hybrid electro-optical systems [9, 10] and in optical tweezers [12, 13].

We have since then combined stable optical levitation in optical tweezers with our optical cavity (Figure 2) and have full control over nanosphere motion even in high vacuum (10^{-7} mbar). Measurements which aim to demonstrate high cooperativity are currently under way, using the scheme on the right of Figure 1. One laser is used to drive the optical cavity and provide (ultimately quantum) control of nanosphere motion ("control mode"),

while the other is orthogonal to the optical cavity and is used solely for suspending the nanosphere in high vacuum ("trapping laser"). High vacuum is needed to improve coherence due to fewer collisions with air molecules (smaller impact of gas heating in decoherence rate Γ). So far we have shown cooperativity $C \approx 10^{-2}$ (publication in preparation).

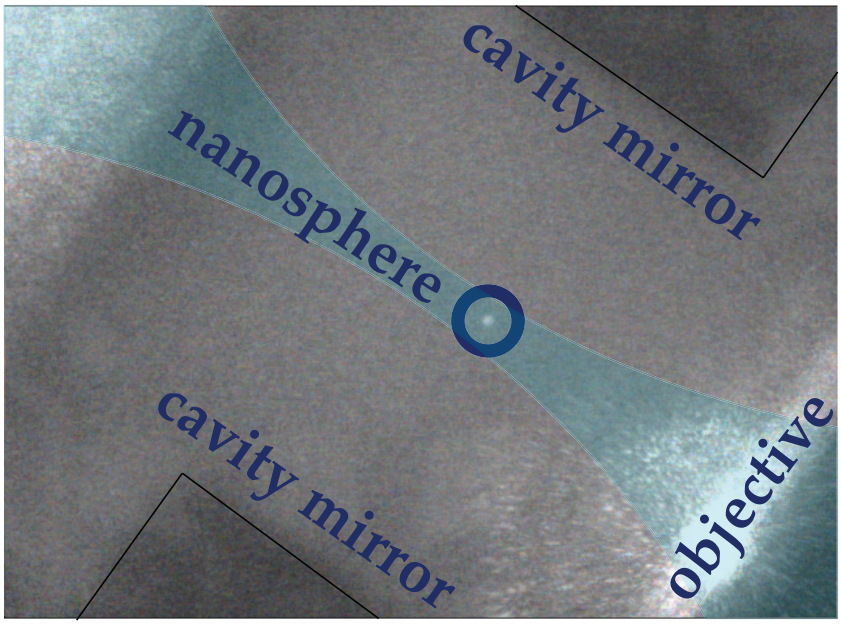

Figure 2: Current view of our experiment. Nanosphere is trapped in an external trapping beam focused by a microscope objective. Objective is sitting on a nanopositioner in order to have full control of nanosphere position in the driven cavity field, defined by two cavity mirrors. In our experiment on coherent scattering, we will aim to prove that just the presence of an empty optical cavity can be enough to have efficient cavity cooling.

We know of several limitations to ultimately reaching a regime of strong cooperativity:

- **Lack of enough laser power.** In practice, control laser is created by passing through a series of optical elements with total efficiency of only $\sim$ 2%. Among several ways to increase optical power, the easiest would be to have a fiber amplifier to increase available power. However, fiber amplifiers add intensity noise to otherwise clean laser sources, possibly impacting our cavity cooling limit (although not directly seen in cooperativity value, which doesn't include all noise sources).

- **Trapping with control laser.** Even with sufficient power in control mode, nanosphere is always trapped in a *total potential*. For example, increasing control mode power will pull nanosphere closer to intensity maximum of cavity mode, thus decreasing linear coupling. We find the optimal position again by repositioning nanosphere until a trap with minimum at cavity intensity slope is created. However, for certain cavity power this starts to be impossible to achieve, as cavity mode becomes the dominant trap laser. In this case, equilibrium trap position will never reach cavity intensity slope again. Possible solution to this problem would be to have **two** cavity modes of equal intracavity powers driving two successive cavity resonances. As intensities of these two modes depend on position x_0 as $\sin^2(kx_0)$ and $\cos^2(kx_0)$ in the vicinity of cavity waist ($x_0 = 0$), total added potential is constant.

- **Recoil heating of cavity mode(s).** Even if we resolve cavity trapping by using two cavity modes, all cavity modes add recoil heating to total decoherence rate Γ. In fact, if we now include all heating rates and attainable couplings, we reach an ultimate cooperativity $C \approx 1.2$. However, we would rather have cooperativity *much* larger than 1.

We have looked into ways how to increase coupling in order to increase cooperativity. This has its limits as recoil heating of cavity modes becomes dominant decoherence mechanism. What about decreasing loss mechanisms instead of only increasing coupling?

- **Cavity energy decay rate κ.** We can easily design a cavity with smaller κ. However, heating due to phase noise depends as $\propto 1/\kappa$, which means there must be an optimal value of κ. We won't go into further discussion here.

- **Recoil heating of trapping laser $\Gamma_{\mathbf{rec}}^{\mathbf{tw}}$.** Both nanosphere mechanical frequency and recoil heating depend on trap intensity I_{tw}. Cavity sideband resolution depends on mechanical frequency, such that higher frequency leads to better cavity cooling. Although trap laser seems to be the one thing we can't change in our setup, it is exactly this we set out to explore in the following text. As we will see below, trap laser can be turned into additional means of cavity cooling of nanosphere motion. This will be cavity cooling by coherent scattering, the topic of our research.

4.2 Current research at the host university

In Vuletić et al. [14] it was proposed that a laser beam orthogonal to an optical cavity could be used in cavity cooling of atom motion, which would make the laser driving the optical cavity obsolete. Light scattered by an atom into the optical cavity could be significantly modified [15] through constructive interference to provide an amplified effect of cavity cooling along the cavity axis. This method has been successfully implemented in the group of Prof. Dr. Vuletić [16], with a recent paper [17] demonstrating three-dimensional cavity ground state cooling of atom gas motion. Currently, experiment is being used to further develop a Bose-Einstein condensate of Cs atoms. It's straightforward to see an analogy to our experiment, as we already have trapping mode driving nanosphere orthogonal to optical cavity. We will explore the case of trapping laser being near to cavity resonance.

5 THEORETICAL WORK

When we couple laser to a cavity through an input cavity mirror, we usually assume a perfect mode matching, i.e. driving laser has the same spatial properties as the cavity mode we drive. Owing to being smaller than laser wavelength ($r \ll \lambda$), nanosphere emits a dipole radiation pattern which doesn't conform to a single Hermite-Gaussian mode. Therefore, only some photons scattered by the nanosphere will continue traveling around cavity in a form of a particular TEM mode, with overall mode matching $\beta \ll 1$. Overlap of scattered photons and a cavity mode in frequency space gives rise to Purcell enhancement of dipole radiation, which will be the topic of this section. In essence, a dielectric nanosphere is equal to an atom cloud with laser being far detuned from any internal atom resonances. Therefore, we use parts of [18] in order to obtain an optomechanical picture of coherent scattering for a scattering nanosphere.

In order to fully understand the effect of coherent scattering from a levitated nanosphere into an optical cavity, we need to develop a full theoretical model. So far, basics of necessary theory have been outlined for atoms [14, 19]. Nanosphere scattering leads to increased cavity decay rate and recoil heating, which has been covered in other work [20, 21, 22]. However, typically only scattering of trapping laser into free modes is considered, hence their definition as losses. Possible scattering into cavity mode (or modes) has been omitted so far, thus no effects of coherent scattering were discussed. Our theoretical study will include, but won't be restricted to:

- Full quantum description of a nanosphere levitated by an external trapping beam, positioned in an optical cavity.
- Mechanism of scattering of external photons into optical cavity. Amplification of scattered light by cavity presence (Purcell effect for nanospheres).
- Exploration of system parameters: magnitude of the effect based on cavity geometry, external trapping beam frequency and polarization, nanosphere size.
- Discussing fundamental experimental steps: calculating magnitude of cavity cooling, detection schemes, impact of optical and acoustic noises on measurements and nanosphere motion.

We ultimately wish to find out if we can cool the nanosphere motion into its ground state with the current experiment at the University of Vienna, possibly with minor modifications to experimental setup. Specific outcome would be a list of measurements we could do to demonstrate the effect of coherent scattering, which would then need to be discussed with the research group at the host university and implemented back at the University of Vienna.

5.1 Overlap of dipole radiation pattern and cavity TEM_{00} mode

As a first step, we need to calculate the amount of light which nanosphere scatters into a mode profile of TEM_{00} cavity mode, which we can do by calculating mode overlap of the dipole radiation mode and TEM_{00} mode field profiles. Dipole radiation pattern of a nanosphere in incident electric field E_{in} at arbitrary distance R is given by:

$$E_{rad}(R,\theta) = \frac{k^2 \sin\theta}{4\pi\epsilon_0}\frac{e^{ikR}}{R}\alpha E_{in}, \tag{4}$$

where θ is angle between polarization of field E_{in} and direction along which E_{rad} propagates. The radiation field is clearly equal to 0 in the direction of E_{in} polarization as $\theta = 0$. This poses a condition on orientation of driving field polarization, which has to be orthogonal to cavity axis ($\theta = \pi/2$) in order to have optimal scattered power toward cavity mirrors. We wish to investigate the mode overlap between a single cavity mode of TEMoo spatial mode profile and the dipole radiation pattern. We assume that the cavity mode has a waist w_0 at cavity center, and $w[L/2]$ at cavity mirror, where L is cavity length. We assume the nanosphere is located at the cavity center, which is a favorable position for strong interaction with any cavity field due to minimal waist. Mode overlap is calculated at cavity mirrors where $R \gg \lambda$, therefore we can use dipole radiation pattern in far-field $e^{ikR}/R = e^{ikx+ik\rho^2/(2x)}/x$. Here x is distance from the nanosphere projected onto cavity axis. The scattering angle θ remains close to $\frac{\pi}{2}$ (on the order of $w[L/2]/L$, which for a realistic confocal cavity is $\sim 10^{-2}$), so we can assume $\sin\theta = 1$.

TEMoo spatial mode is given by:

$$E_{00} = E_0 \frac{w_0}{w[x]} \exp\left(-\frac{\rho^2}{w^2[x]}\right) \exp^{-ikx-\frac{ik\rho^2}{2x}}, \tag{5}$$

where $w[x] = w_0\sqrt{1+(x/x_R)^2}$. Overlap of two modes is:

$$\begin{aligned}
\frac{1}{E_{in}E_0}\int_0^{2\pi}\int_0^{\infty} E_{00}E_{rad}\rho d\rho d\varphi &= \frac{k^2\alpha}{2\epsilon_0}\frac{w_0}{w[x]x}\int_0^{\infty} e^{-\frac{\rho^2}{w^2[x]}}\rho d\rho = \\
\frac{k^2\alpha}{2\epsilon_0}\frac{w_0}{x}\frac{-w[x]}{2}\int_0^{\infty} e^{-\frac{\rho^2}{w^2[x]}} d\left(-\frac{\rho^2}{w[x]^2}\right) &= \frac{k^2\alpha}{2\epsilon_0}\frac{-w_0 w[x]}{2x} e^{-\frac{\rho^2}{w^2[x]}}\Big|_0^{\infty} = \\
\frac{k^2\alpha}{2\epsilon_0}\frac{-w_0 w[x]}{2x}\left(\lim_{\rho\to\infty} e^{-\frac{\rho^2}{w^2[x]}} - e^{-\frac{0}{w^2[x]}}\right) &= \frac{k^2\alpha w_0}{4\epsilon_0}\frac{w[x]}{x}.
\end{aligned} \tag{6}$$

At distances x greater than Rayleigh range $x_R = \frac{w_0^2\pi}{\lambda}$, mode overlap normalized over an effective mode area of the cavity mode $A = \pi w_0^2/2$ is:

$$\beta = \frac{1}{A}\frac{1}{E_{in}E_0}\int_0^{2\pi}\int_0^{\infty} E_{00}E_{rad}\rho d\rho d\varphi = \frac{k\alpha}{\epsilon_0 w_0^2\pi}. \tag{7}$$

It is compelling to see if there is a significant mode overlap when polarization of E_{in} is collinear to TEMoo axis, i.e. $\theta \approx 0$. Following the same procedure with new condition of $\sin\theta \approx \tan\theta = \frac{\rho}{L/2}$, we still get a non-zero mode overlap:

This time it's necessary to integrate by parts with $du = e^{-\frac{\rho^2}{w^2}}\rho\, d\rho$ and $v = \rho$.

$$\beta_{min} = \frac{\alpha}{\varepsilon_0 w_0^3\sqrt{\pi}}. \tag{8}$$

In the case of our near-confocal cavity with $w_0 \approx 40\times10^{-6}\mu m$, $\frac{\beta}{\beta_{min}} \sim 100$. Scattered power is $\propto |\beta|^2$, hence scattering is suppressed by at least a factor of 10000 by fine tuning polarization of driving field.

Electric field scattered into a TEMoo mode defined by our cavity is:

$$E_M = i\beta E_{in}, \tag{9}$$

where $|E_{in}|^2 = \frac{2I_{in}}{\varepsilon_0 c} = \frac{P_{in}k^2NA^2}{\varepsilon_0 c\pi}$ is electric field of optical tweezers. Imaginary unit i shows up due to Gouy phase $\pi/2$ of cavity mode at distances $x \gg x_R$. It is important to note that this equation holds for any drive electric field independent of mode shape, with only condition being that scattered field lies in a plane orthogonal to light polarization.

Optical power scattered into one half of a cavity mode E_M is $P_M = |\beta|^2 P_{in}k^2w_0^2NA^2/4$. Total dipole emitted power is determined by integrating intensity $I_{rad} = \varepsilon_0 c|E_{rad}|^2/2$ over the surface of a sphere with arbitrary radius R:

$$P_{4\pi} = \frac{ck^4}{12\pi\varepsilon_0}|\alpha E_{in}|^2 = \frac{k^2w_0^2}{3}|\beta|^2\frac{P_{in}k^2w_0^2NA^2}{4}. \tag{10}$$

Ratio of light scattered into modes E_M and scattered into whole space is called free space cooperativity:

$$\eta_{fs} = \frac{2P_M}{P_{4\pi}} = \frac{6}{k^2w_0^2}. \tag{11}$$

Factor of 2 accounts for scattering into both directions of a TEMoo mode, such that cavity would collect light scattered into fraction of solid angle η_{fs}.

5.2 Enhanced scattering due to cavity

Scattered light into mode E_M can bounce many times between the mirrors and interfere with itself, leading to a myriad of interesting optical and optomechanical effects. Left-traveling field E_M will reflect once from mirror M1 and interfere with field E_M scattered in the direction of mirror M2 (Figure). Considering a case when built-up "right traveling" cavity electric field is much smaller than driving field ($E_{c,r} \ll E_{in}$), field $E_{c,r}$ reached in equilibrium depends on relative phase shift between scattered fields:

$$E_{c,r} = E_M + r_1 e^{ik(L+2\Delta x)} E_M + r_1 r_2 e^{2ikL} E_{c,r}, \tag{12}$$

where r_1^2, r_2^2 are mirror reflectivities and Δx is nanosphere distance from cavity center along cavity axis. Note that we have taken accumulated phase shift to be positive in traveled distance for this right traveling wave. As we will see in later text, this will coincide with quantization of cavity mode.

Our experimental cavity is designed to be symmetric, hence we can take $|t_1|^2 = |t_2|^2$ and $|r_1|^2 \approx |r_2|^2$. However, we continue using r_1 and r_2 without any assumption on their relative values. E_M is electric field scattered in the direction of mirror M2, while $r_1 e^{ik(L+2\Delta x)} E_M$ is light scattered in opposite direction and reflected from mirror M1. We can solve this for $E_{c,r}$:

$$E_{c,r} = i\beta E_{in} \frac{1 + r_1 e^{ikL} e^{2ik\Delta x}}{1 - r_1 r_2 e^{2ikL}}. \tag{13}$$

Let's look into a simple case of laser being resonant with the cavity, i.e. $e^{2ikL} = 1$. Without a loss in generality, we can assume $e^{ikL} = 1$, thus choosing that the cavity standing wave has its maximum at the cavity waist. Cavity electric field becomes:

$$E_{c,r} = i\beta E_{in} (1 + r_1 e^{2ik\Delta x}) \frac{\mathcal{F}}{\pi}, \tag{14}$$

where we have used known definition of cavity finesse $(1 - r_1 r_2)^{-1} = \mathcal{F}/\pi$. Power of the right traveling electric field is:

$$P_{c,r} = \frac{|E_{c,r}|^2}{2\varepsilon_0 c} \frac{w_0^2 \pi}{2} = I_{in} \frac{w_0^2 \pi}{2} |\beta|^2 \left(\frac{\mathcal{F}}{\pi}\right)^2 \left(1 + r_1^2 + 2r_1 \cos(2k\Delta x)\right). \tag{15}$$

It clearly depends on nanosphere position through $\cos(2k\Delta x)$, where distance Δx is a combination of equilibrium trap position x_0 and nanosphere COM motion $x(t)$, although we neglect fluctuations caused by nanosphere motion for now. Assuming nanosphere is sitting at the intensity maximum ($\cos(2kx_0) = 1$) and $r_1 \approx 1$, cavity power would approximately be:

$$P_{c,r} = P_{in} k^2 w_0^2 NA^2 |\beta|^2 \left(\frac{\mathcal{F}}{\pi}\right)^2. \tag{16}$$

It is clear that although only a small fraction of trap laser is reflected into the cavity mode ($\propto |\beta|^2 P_{in}$), power in the cavity is amplified by a huge factor depending on cavity finesse $\left(\frac{\mathcal{F}}{\pi}\right)^2$.

With detuned drive $\omega_l = \omega_c - \Delta$, resonance condition turns into $e^{2ikL} = e^{-i\Delta/\Delta\nu_{FSR}}$. Thus:

$$\frac{1}{|1 - r_1 r_2 e^{2ikL}|^2} \approx \frac{1}{\left|1 - r_1 r_2 \cos\frac{\Delta}{\Delta\nu_{FSR}} + i r_1 r_2 \sin\frac{\Delta}{\Delta\nu_{FSR}}\right|^2} \approx \frac{(\mathcal{F}/\pi)^2 \left(\frac{\kappa}{2}\right)^2}{\left(\frac{\kappa}{2}\right)^2 + \Delta^2},$$

where we see that cavity amplification is reduced by the cavity transfer function.

PURCELL FACTOR. Small portion of $P_{c,r}$ leaks out of the cavity through mirror M2: $P_2 = |t_2|^2 P_{c,r}$. As transmission through M2 attributes to half of the cavity photon loss, we can express it through cavity finesse as $|t_2|^2 \approx \pi/\mathcal{F}$, hence:

$$P_2 = P_{in} k^2 w_0^2 N A^2 |\beta|^2 \frac{\mathcal{F}}{\pi}. \tag{17}$$

If we compare the total power leaked through cavity mirrors with the power dipole emitted into the whole space $P_{4\pi}$, we obtain what is commonly regarded as Purcell factor [23] of enhancement η:

$$\eta = \frac{P_1 + P_2}{P_{4\pi}} = 4\frac{\mathcal{F}}{\pi}\eta_{fs} = \frac{24\mathcal{F}/\pi}{k^2 w_0^2}. \tag{18}$$

Therefore, although cavity takes only a small solid angle of whole dipole radiation, it stimulates the radiation in the cavity direction such that we have an overall enhancement. As shown in [18], Purcell factor of dipole interaction is equal to atomic cooperativity obtained from quantum treatment.

5.3 Modified enhanced scattering into cavity

All of the effects seen so far still don't fall into the category of cavity optomechanics, such as cavity cooling or optical spring and damping. These effects come into play only in a case of strong amplification of field E_M in the cavity. In that case, not only do we get interference of E_M terms, but we also have to take into account light scattered from built-up intracavity fields $E_{c,r}$ and $E_{c,l}$ as $E_M = i\beta(E_{in} + E_{c,r} + E_{c,l})$. Left travelling and right travelling fields $E_{c,l}$ and $E_{c,r}$ are related by a phase $E_{c,l} \approx E_{c,r} e^{ik(L-2\Delta x)}$, such that with a change of notation $E_{c,r} = E_c$:

$$E_c = r_1 r_2 e^{2ikL} E_c + i\beta \left(E_{in} + E_c \left(1 + r_2 e^{ik(L-2\Delta x)}\right)\right)\left(1 + r_1 e^{ik(L+2\Delta x)}\right). \tag{19}$$

We assume drive with arbitrary detuning, $e^{ikL} \approx 1$ and that mirror reflectivities are $r_1^2, r_2^2 \approx 1$:

$$\begin{aligned} E_c &= \frac{i\beta E_{in}\left(1 + e^{2ik\Delta x}\right)}{1 - r_1 r_2 + i\frac{\Delta}{\Delta\nu_{FSR}} - i4\beta\cos^2 k\Delta x} \\ &= \frac{i\beta\Delta\nu_{FSR} E_{in}\left(1 + e^{2ik\Delta x}\right)}{\frac{\kappa'}{2} + i\Delta'}, \end{aligned} \tag{20}$$

where we have introduced modified cavity FWHM κ' and detuning Δ' as:

$$\begin{aligned} \kappa' &= \kappa + 8\,\mathrm{Im}(\beta)\Delta\nu_{FSR}\cos^2 k\Delta x, \\ \Delta' &= \Delta - 4\,\mathrm{Re}(\beta)\Delta\nu_{FSR}\cos^2 k\Delta x. \end{aligned}$$

$\mathrm{Re}(\beta)\Delta\nu_{FSR}$ is a recurring factor which is equal to $U_0/4$, where $U_0 = \frac{3}{2}\frac{\omega_l V}{V_{cav}}\,\mathrm{Re}\left(\frac{n^2-1}{n^2+2}\right)$ is nanosphere-induced frequency shift. Note following effects which rise from (20):

1. **Modified cavity FWHM.** Nanosphere scatters light out of the cavity and thus modifies the total cavity energy decay rate (full width - half maximum, FWHM) by $\kappa_{scatt} = 8\,\mathrm{Im}(\beta)\Delta\nu_{FSR}\cos^2 kx_0$, depending on trap position x_0. Scattering rate is a function of $\mathrm{Im}(\beta)$:

$$\mathrm{Im}(\beta) = |\beta|^2 \frac{1}{\eta_{fs}} = \left(\frac{k|\alpha|}{\varepsilon_0 w_0^2 \pi}\right)^2 \frac{k^2 w_0^2}{6} \propto r^6. \tag{21}$$

2. **Modified detuning by a constant frequency.** Nanosphere has a different refractive index compared to the environment, thus changing the cavity resonant frequency by $U(x) = U_0 \cos^2 kx_0$. It is a constant offset to detuning Δ with $U_0 \ll \Delta$. It is irrelevant to our experiment as we either keep laser resonant to cavity or we can manually change detuning to desired value if nanosphere moves to a different position.

3. **Linear coupling to cavity mode.** Nanosphere induces a position-dependent frequency shift to the cavity resonance with rate U_0:

$$\frac{\partial \omega_c}{\partial x} = -U_0 k \sin 2kx_0 = -\frac{g_0}{x_{zpf}} \sin 2kx_0. \tag{22}$$

4. **Position dependent drive term.** Input field coupling $1 + e^{2ik\Delta x}$ to cavity obviously depends on nanosphere position Δx, where we have previously made an assumption of "stationary nanosphere", i.e. $\Delta x = x_0$. We will look in detail what is the impact of including nanosphere motion $x(t)$ in this coupling term further in this chapter.

Points $1-3$ show up in conventional (as in: driving cavity through cavity mirror) cavity optomechanics with levitated nanospheres as well. Therefore, we first seek to apply this formalism to a case of cavity driven through one of the mirrors and confirm its practicality. It's clear that point 4 will lead to additional effects, such as coherent scattering. This we will see after our brief excursion in the following text.

5.3.1 *Cavity driven through a cavity mirror*

Let us look into a case where we drive the cavity through one of the input mirrors, e.g. mirror M1. We can apply the formalism used in driving by trapping laser in order to calculate the right traveling cavity field. We start with cavity input, where only a fraction of input field $t_1 \beta E_{in}^{M1}$ transmits through the input mirror. We assume perfect mode matching of input field E_{in}^{M1} and driven cavity mode $E_{c,r}$, i.e. $\beta = 1$. In equilibrium, created cavity electric field satisfies following relation at trap position Δx:

$$\begin{aligned} E_{c,r} &= r_1 r_2 e^{2ikL} E_{c,r} + t_1 E_{in}^{M1} e^{ik(\frac{L}{2}+\Delta x)} \\ &+ i\beta E_{c,r} \left(1 + r_2 e^{ik(L-2\Delta x)}\right) \left(1 + r_1 e^{ik(L+2\Delta x)}\right). \end{aligned} \tag{23}$$

We include phase factor $e^{ik(\frac{L}{2}+\Delta x)}$ to account for phase accumulated between input mirror and trap position, which is important in order to be able to later implement proper quantization of $E_{c,r}$. Through a direct comparison with (19), we already see that the nanosphere can be thought of as an input mirror with "transmission coefficient" β in the case of coherent scattering. Although $\beta \ll t_1$, drive intensity I_{in} is typically orders of magnitude higher than I_{in}^{M1} due to tighter focus and larger powers needed to trap a nanosphere. Hence, the drive can be considerably stronger in the case of coherent scattering.

Without any loss in generality, we can again set $e^{ikL} \approx 1$ and $r_1, r_2 \approx 1$. As we're working with traveling waves, it's useful to apply notation of quantized traveling waves. We are not working with cavity standing wave per se, although boundary conditions will still apply. Right and left traveling waves are defined as [24]:

$$\begin{aligned} E_r &\propto i\sqrt{\frac{\hbar\omega_l}{2\varepsilon_0 V_{cav}}} \left(\hat{a} e^{ikx} e^{-i\omega_l t} - \hat{a}^\dagger e^{-ikx} e^{i\omega_l t}\right) \\ E_l &\propto -i\sqrt{\frac{\hbar\omega_l}{2\varepsilon_0 V_{cav}}} \left(\hat{a} e^{-ikx} e^{-i\omega_l t} - \hat{a}^\dagger e^{ikx} e^{i\omega_l t}\right). \end{aligned}$$

It is clear that our convention of positive phase shifts was related only to half of quantized field E_r which is proportional to annihilation operator $\hat{a}$. By choosing negative phase shifts e^{-ikx}, we would have ended up with an equation governing the evolution of creation operator $\hat{a}^\dagger$. Note that total electric field $E_t = E_r + E_l \propto 2\left(\hat{a}e^{-i\omega_l t} + \hat{a}^\dagger e^{i\omega_l t}\right)\sin kx$, in agreement with usual cavity mode quantization. It is important to choose a correct coordinate system for propagation of traveling waves, which is commonly chosen to be at the input cavity mirror. Therefore, we have to displace electric field $E_{c,r}$ by $e^{il\left(\frac{L}{2}+\Delta x\right)}$ in order to obtain E_r, where it's obvious why we had to include correct phase shifts in $E_{c,r}$. Although it seems like a simple and unnecessary trick, this will be especially important when we try to quantize electric field generated by coherent scattering.

Nothing stops us now from writing a quantum Langevin equation for operator $\hat{a}$:

$$\dot{\hat{a}} = -\left(\frac{\kappa'}{2} + i\Delta\right)\hat{a} + E_d - iU_0 k\hat{a}\hat{x}\sin 2kx_0, \tag{24}$$

$\kappa_1 = t_1^2 \Delta\nu_{FSR}$

where $E_d = t_1 E_{in}\Delta\nu_{FSR}\sqrt{\frac{2\varepsilon_0 V_{cav}}{\hbar\omega_l}} = \sqrt{\frac{P_{in}\kappa_1}{\hbar\omega_l}}$. This equation is in complete agreement with Langevin equations of levitated optomechanics. Therefore, employing classical theory of dipole scattering can lead us to describing quantum evolution of our system by light quantization as the final step. Although we haven't written an equation for $\hat{x}$, we now go back to the case of coherent scattering and investigate quantum evolution of $\hat{a}$.

5.4 Quantum Langevin equations of motion for coherent scattering

Field E_c in (20) is right traveling field at the nanosphere trap position. In order to implement quantization correctly, we need to calculate electric field at cavity center, which serves as coordinate system origin:

$1 + e^{2ik\Delta x} \to e^{-ik\Delta x} + e^{-ik\Delta x} = 2\cos k\Delta x$

$$\dot{\hat{a}} = -\left(\frac{\kappa'}{2} + i\Delta'\right)\hat{a} + iE_d\cos(kx_0) - iE_d k\sin(kx_0)\hat{x} - iU_0 k\sin(2kx_0)\hat{x}. \tag{25}$$

We at once spot an additional linear coupling to mechanics with $g'(x_0) = E_d k x_{zpf}\sin(kx_0)$, which behaves differently on x_0 compared to coupling $g(x_0) = g_0\alpha_0\sin(2kx_0)$. If we look into periodicity (Figure 3), we see that new coupling is to cavity electric field, compared to usual optomechanical coupling. This is a regime yet unexplored in sideband resolved cavity optomechanics as no other can scatter external field into a cavity mode. However, driving field detuned far away from atom resonance can generate significant cooling force, although atoms exhibit Doppler cooling rather than sideband cooling due to small trap frequencies. This has already been demonstrated in detail in [25].

In analogy to driving cavity through one of the mirrors, we define input drive $E_d = \sqrt{\frac{P'_{in}\kappa_{nano}}{\hbar\omega_l}}$ with input κ_{nano}:

$$\kappa_{nano} = 4|\beta|^2\Delta\nu_{FSR}. \tag{26}$$

Power $P'_{in} = I_{in}\frac{w_0^2\pi}{2}$ is driving power rescaled to cavity mode with waist w_0, i.e. I_{in} is laser intensity shining on nanosphere from the side of cavity. There is a relation between κ_{nano} and $\kappa_{scatt}^{max} = 8\,\mathrm{Im}(\beta)\Delta\nu_{FSR}$:

$$\kappa_{nano} = \frac{\kappa_{scatt}}{2}\eta_{fs}, \tag{27}$$

where we have already seen η_{fs} as cavity mode-to-free space ratio of light scattering. This shows that while κ_{scatt} is scattering the cavity light into

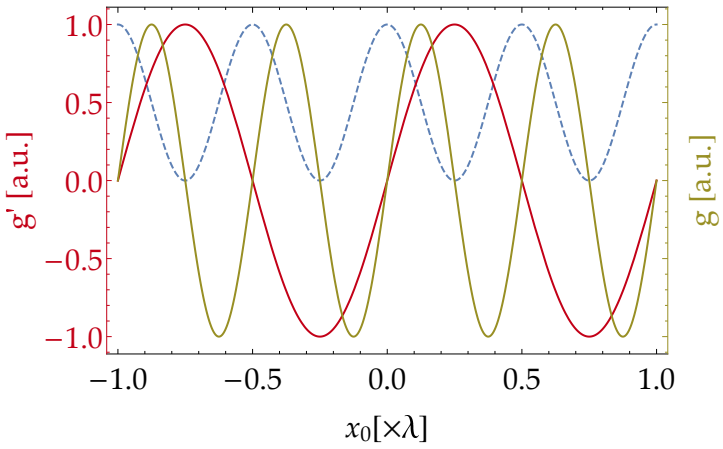

Figure 3: Comparison of linear coupling g_0 to standing wave intensity (green) to additional linear coupling g_0' to standing wave electric field (red). Cavity standing wave intensity profile is plotted for reference (dashed, blue), which shows maximum amplitudes of g_0' at cavity nodes. g_0 has its maximum amplitudes at maximum slopes of intensity profile. $x_0 = 0$ is position of cavity center, where we have intensity maximum.

whole space, the rate of reverse process driving the cavity mode is η_{fs} ratio of it.

Usually we have a case $\kappa_{nano} \ll \kappa_1$, as mode overlap is small for large cavity waists $|\beta|^2 \ll |t_1|^2$. However, field intensity I_{in} in case of coherent scattering is orders of magnitude larger than in the case of driving through the cavity mirror. Ratio comes from higher total power needed to use in trapping a nanosphere (up to a factor of 100), as well as from ratio of effective mode areas (factor of about $k^2 w_0^2$) of tweezer and cavity modes, which can bridge another 3-4 orders of magnitude. For a cavity waist of $w_0 = 10$ μm, we can already have comparable drive to a drive through a 10 ppm input mirror. Intracavity photon number is given by E_d^0:

$$n_{phot} = |\alpha_0|^2 = \frac{E_d^2 \cos^2(kx_0)}{\left(\frac{\kappa'}{2}\right)^2 + \Delta^2}. \tag{28}$$

We assume no additional drive through a cavity mirror.

Under assumption of large coherent amplitude of cavity field ($\hat{a} \approx \alpha_{ph}$), we combine terms containing $\hat{x}$:

$$\begin{aligned} \dot{\hat{a}} &= -\hat{a}\left(\frac{\kappa'}{2} + i\Delta\right) - i\frac{g(x_0) + g'(x_0)}{x_{zpf}}\hat{x} \\ &+ \sqrt{\kappa_{IN}}(\hat{a}_{IN}^1 + \hat{a}_{IN}^2) + \sqrt{\kappa_{nano}\cos^2(kx_0)}\hat{a}_{TW}. \end{aligned} \tag{29}$$

It's interesting to compare amplitudes of $g'(x_0)$ and $g(x_0)$, assuming intracavity amplitude α_0:

$$\frac{\max(g')}{\max(g)} = \frac{E_d}{U_0\alpha_0} = \frac{\sqrt{\left(\frac{\kappa'}{2}\right)^2 + \Delta^2}}{U_0}, \tag{30}$$

where we see our detection of $\hat{x}$ motion can be significantly improved even for a resonant cavity. The reason $g' > g$ is twofold:

- **Large cavity waist.** Although frequency shift $U_0 \propto w_0^{-2}$ and $E_d \propto w_0^{-2}$, cavity amplitude $\alpha_0 \propto w_0^{-2}$ as well. For our waist of near-confocal cavity $w_0 = 41$ μm and at resonant drive $\Delta = 0$, $g'/g \approx 6$. If we use a different cavity design and attain a waist ~ 16 μm, ratio $g'/g \to 1$.

- **Small cavity finesse.** With better mirrors we could hope to get $\kappa \sim 2\pi \times 50$ kHz, which shifts the limit of minimal ratio g'/g to chosen detuning as $\Delta \gg \kappa/2$.

- **High trap intensity.** Due to high trap intensity, we win in comparison to driving cavity through a mirror. We expect a trap waist $w_0 = \frac{\lambda}{\pi NA} \approx 0.4\mu m$ from numerical aperture $NA = 0.8$, however we characterize the waist to be around $w_0 \approx 1\mu m$, probably due to an imperfect overfilling of microscope objective.

.

6 QUANTUM DESCRIPTION

We might ask a question: what is fundamentally different in this experimental setup compared to the setup discussed in our previous work? It's easy to notice that we are not driving the cavity through one of the input mirrors, but by enhanced light scattering into the cavity mode. How is the drive then described in this setup?

In previous work published on levitated optomechanics, an interference term between E_{tw} and E_{cav} was defined to be zero due to orthogonal polarizations. For the coherent scattering to work, we have to rotate tweezer laser polarization by 90° in order to have favorable scattering into the direction of cavity mirrors. Hence, it's possible to have equal polarizations of trapping and cavity mode, giving rise to interference term $\propto E_{tw}E_{cav}$, which we investigate in detail. We aim to reproduce effects seen in classical formalism presented earlier in this text.

6.1 Interaction between tweezer and cavity modes

We remind ourselves that dipole interaction Hamiltonian reads:

$$\hat{H}^i_{light-nano} = -\frac{1}{2}\alpha\left|\vec{E}\right|^2 = -\frac{1}{2}\alpha\left|\vec{E}_{cav} + \vec{E}_{tw} + \vec{E}_{free}\right|^2,$$

where we can forget about free modes for now. We have already defined terms $\propto \left|\vec{E}_{tw}\right|^2$ and $\propto \left|\vec{E}_{cav}\right|^2$ as being responsible for levitation and optomechanics, respectively. We have neglected cross-term $\vec{E}_{cav}\vec{E}_{tw}$ in the past, as we could tweak them to have orthogonal polarizations. However, let's now loosen this condition and assume the two electric fields to have equal polarization:

$$\hat{H}^i_{cav-tw} = -\frac{1}{2}\alpha\left(E_{tw}E^*_{cav} + E^*_{tw}E_{cav}\right).$$

If we apply quantization of cavity modes to this Hamiltonian, we get a familiar expression:

$$\hat{H}^i_{cav-tw} = -\frac{1}{2}\alpha\epsilon E_{tw}\left(\hat{a}^\dagger f^*(\vec{r})e^{-i\omega_{tw}t} + \hat{a}f(\vec{r})e^{i\omega_{tw}t}\right), \tag{31}$$

where $\epsilon = \sqrt{\frac{\hbar\omega_c}{2\varepsilon_0 V_{cav}}}$ is electric field per photon and $|f(\vec{r})|^2$ is cavity intensity profile. Eq.(31) resembles the Hamiltonian of drive cavity field in Eq.(**??**) with $E_d = \alpha\epsilon E_{tw}/2\hbar$, with an exception that the drive field now depends on the position of "input mirror", i.e. nanosphere. To keep things simple, we assume nanosphere is on the cavity axis at an arbitrary position x_0, such

that $f(\vec{r}) = \cos k\Delta x = \cos k(x_0 + x(t))$. We go into the rotating frame picture and hold on to terms which contain operators $\hat{a}$ and $\hat{a}^\dagger$ only:

$$\frac{\hat{H}^i_{l-n}}{\hbar} = -\underbrace{U_0 \cos^2 k\Delta x \hat{a}^\dagger \hat{a}}_{\text{from } E^2_{cav}} - \underbrace{E_d \cos k\Delta x \left(\hat{a}^\dagger + \hat{a}\right)}_{\text{from } E_{cav} E_{tw}} - \underbrace{\frac{m\omega_0^2 \hat{x}^2}{2\hbar}}_{\text{from } E^2_{tw}}, \tag{32}$$

with total Hamiltonian $\hat{H} = \hbar\Delta\hat{a}^\dagger\hat{a} + \hat{H}^i_{l-n}$. Assuming we can decompose $\hat{a}$ into a sum of its coherent and noise part $\hat{a} \to \alpha_0 + \hat{a}$, first two terms in Eq.(32) can be explained in the following way:

- $U_0 \cos^2 k\Delta x \hat{a}^\dagger \hat{a}$ leads to always-present optomechanical interaction term $\hat{H}^1_{OM} = \hbar U_0 k |\alpha_0| \sin(2kx_0)\hat{x}\left(\hat{a}^\dagger + \hat{a}\right)$ and shift to cavity frequency $\Delta' = \Delta - U_0 \cos^2 kx_0$.
- $E_d \cos k\Delta x \left(\hat{a}^\dagger + \hat{a}\right)$ will hold additional, previosly undescribed optomechanical interaction $\hat{H}^2_{OM} = \hbar E_d k \sin(kx_0)\hat{x}\left(\hat{a}^\dagger + \hat{a}\right)$.

Two interaction terms $\hat{H}^1_{OM}$ and $\hat{H}^2_{OM}$ happen to have different dependencies on trap position x_0. Due to nanosphere's coupling to the intensity, $\hat{H}^1_{OM}$ depends on standing wave mode function, while we can see that $\hat{H}^2_{OM}$ rather describes coupling to electric field of cavity mode, hence different periodicity conditions apply. In analogy to Chapter **??** we define total coupling $g(x_0) = E_d k x_{zpf} \sin(kx_0) + U_0 k x_{zpf} |\alpha_0| \sin(2kx_0)$. In the case of large waists of near-confocal cavities, interaction through $\hat{H}^2_{OM}$ is much stronger than $\hat{H}^1_{OM}$ due to weakly populated cavity mode amplitude $|\alpha_0|$ and high tweezer intensity I_{tw}. We admit that $|\alpha_0|$ can be significantly increased by driving cavity through a cavity mirror, however here we focus solely on driving through nanosphere, as this will lead to many interesting and favorable effects. We could increase U_0 by decreasing cavity mode volume V_c ($U_0 \propto \frac{1}{V_c}$), however this would include designing cavities with smaller waists, which tend to be hard to align or unstable to use. In order to further explore system dynamics, we write Langevin equations:

$$\begin{aligned}
\dot{\hat{p}} &= -m\omega_0^2\hat{x} - \gamma_m\hat{p} - \hbar U_0 k \sin(2kx_0)\hat{a}^\dagger\hat{a} - \hbar E_d k \sin(kx_0)\left(\hat{a}^\dagger + \hat{a}\right) \\
&+ F_{th}(t) \\
\dot{\hat{x}} &= \frac{\hat{p}}{m} \\
\dot{\hat{a}} &= -\left(\frac{\kappa}{2} + i\Delta'\right)\hat{a} - i\left(U_0 \sin(2kx_0)\hat{a} + E_d \sin(kx_0)\right)k\hat{x} \\
&+ iE_d \cos(kx_0) + \sqrt{\kappa_{nano}}\hat{a}_{tw} + \sqrt{\kappa_{in}}\left(\hat{a}^1_{IN} + \hat{a}^2_{IN}\right).
\end{aligned} \tag{33}$$

Loss-rate κ_{nano} is given by:

$$\kappa_{nano} = \tag{34}$$

By moving into displaced frame $\hat{a} \to \alpha_0 + \hat{a}$, we shift light operators by amplitude α_0:

$$\alpha_0(x_0) = \frac{iE_d \cos kx_0}{\frac{\kappa}{2} + i\Delta'} \tag{35}$$

Here we see how cavity field comes into existence through scattering of tweezer light into cavity mode. Intracavity photon number $n_{phot} = |\alpha_0|^2$ equals the value obtained in classical formalism earlier in this chapter. Coupling of $\hat{x}$ to cavity electric field is larger than coupling to intensity by $\sqrt{(\kappa/2)^2 + \Delta'^2}/U_0$. This ratio rises from the fact of how well nanosphere scattered light is coupled to the cavity mode, either by overlap of scattered light and cavity mode through U_0 or by amplification of scattered light, which depends on κ and Δ. Interestingly, maximum coupling to electric field is reached when $\sin(kx_0) = \pm 1$, which implicates that $\alpha_0 = 0$, i.e. no

intracavity field is created. Therefore, there won't be any added recoil heating from a cavity mode. Total coupling $g(x_0)$ and mechanical frequency $\omega_0'(x_0)$ are plotted in comparison to changes induced by regular optomechanical effects in Figure 3. We assume coherent amplitude α_0 as given by Eq. (35).

After operator displacement and keeping only lowest-order terms, Langevin equation of operator $\hat{a}$ is simplified into:

$$\dot{\hat{a}} = -\left(\frac{\kappa}{2} + i\Delta'\right)\hat{a} - i\frac{g(x_0)}{x_{zpf}}\hat{x} + \sqrt{\kappa_{nano}}\hat{a}_{tw} + \sqrt{\kappa_{in}}\left(\hat{a}_{IN}^1 + \hat{a}_{IN}^2\right) \tag{36}$$

Taking into account displacement of $\hat{a}$, Langevin equations describing mechanics are unified into a single equation:

$$\ddot{\hat{x}} + \gamma_m\dot{\hat{x}} + \omega_0^2\hat{x} - \frac{\hbar g(x_0)}{x_{zpf}}\left(\hat{a}^\dagger + \hat{a}\right) = f_{th}(t). \tag{37}$$

From now on, we can follow the usual procedure of solving a system of Langevin equations for operators $\hat{a}$ and $\hat{x}$, which brings us to the usual cavity optomechanical cooling [26].

6.1.1 *Coupling to motion along y*

Rotation of tweezer linear polarization by angle α leads to rotation of oscillation x-y plane by 2α, without any change to oscillation frequencies. We mark these new oscillation axes as u and v, such that their projections along cavity axis x and its orthogonal axis y are:

$$x = u\cos 2\alpha + v\sin 2\alpha, \qquad y = u\sin 2\alpha - v\cos 2\alpha. \tag{38}$$

Rotation by $\alpha = 22.5°$ will allow for equal coupling of both oscillation axes to cavity mode. Although this will clearly allow for cavity cooling of motion projection along cavity axis, it's not apparent if we can cool both directions.

At optimal position of $\sin(kx_0) = 1$ for cavity cooling by coherent scattering, Hamiltonian $\hat{H}_{OM}^2$ has the form of:

$$\hat{H}_{OM}^2 = \frac{\hbar E_d k}{\sqrt{2}}(\hat{u} + \hat{v})\left(\hat{a}^\dagger + \hat{a}\right). \tag{39}$$

System dynamics is described by following Langevin equations:

$$\begin{aligned}
\ddot{\hat{u}} + \gamma_m\dot{\hat{u}} + (\omega_0^u)^2\hat{u} - \frac{\hbar E_d k}{\sqrt{2}m}\left(\hat{a}^\dagger + \hat{a}\right) &= f_{th}^u \\
\ddot{\hat{v}} + \gamma_m\dot{\hat{v}} + (\omega_0^v)^2\hat{v} - \frac{\hbar E_d k}{\sqrt{2}m}\left(\hat{a}^\dagger + \hat{a}\right) &= f_{th}^v \\
\dot{\hat{a}} + \left(\frac{\kappa}{2} + i\Delta\right)\hat{a} - i\frac{E_d k}{\sqrt{2}}(\hat{u} + \hat{v}) &\approx 0
\end{aligned} \tag{40}$$

Assuming $\omega_0^u = \omega_0^v$, difference of first two equations ends up in a differential equation for $\hat{y}$, which doesn't include operators $\hat{a}$ and $\hat{a}^\dagger$. However, for $\omega_0^u \neq \omega_0^v$, it is impossible to obtain a differential equation for $\hat{y}$ which doesn't include cavity influence. Therefore, one can cool both directions only in the case that oscillation frequencies are non-degenerate.

Solving this system of equation involves Fourier transforms again and yields cavity cooling of both x and y-motion.

6.1.2 *Coupling to motion along z*

Phase of scattered light will depend on motion of the nanosphere along the tweezer axis z as well. In the Lamb-Dicke regime ($k\langle z\rangle \ll 1$), $e^{ikz} \approx 1 + ikz$, so:

$$\hat{a}^\dagger + \hat{a} \to \left(\hat{a}^\dagger + \hat{a}\right) + ikz\left(\hat{a}^\dagger - \hat{a}\right). \tag{41}$$

As a first order approximation, we can expand Langevin equation for operator $\hat{a}$ as:

$$\begin{aligned}\dot{\hat{a}} &= -\left(\frac{\kappa}{2}+i\Delta'\right)\hat{a} - i\frac{g(x_0)}{x_{zpf}}\hat{x} - E_d k\cos(kx_0)\hat{z} \\ &+ \sqrt{\kappa_{nano}}\hat{a}_{tw} + \sqrt{\kappa_{in}}\left(\hat{a}^1_{IN}+\hat{a}^2_{IN}\right). \end{aligned} \tag{42}$$

We can write a Langevin equation for $\hat{z}$ as well:

$$\ddot{\hat{z}} + \gamma_m\dot{\hat{z}} + (\omega_0^z)^2\hat{z} - i\frac{\hbar E_d k}{m}\cos(kx_0)\left(\hat{a}^\dagger - \hat{a}\right) = f^z_{th}(t). \tag{43}$$

From these equations we see that if we wish to see any effect of cavity cooling of z-motion, trap position needs to satisfy $\cos(kx_0) \neq 0$, in clash with optimal trap position for cooling of x motion [**?**]. In the optimal case of $\cos(kx_0) = 1$, coupling to x motion is minimized, while coupling to z motion is optimal. In this configuration, Langevin equations are solved by Fourier transform:

$$\tilde{z}\left((\omega_0^z)^2 - \omega^2 + i\gamma_m\omega - i\frac{\hbar(E_d k)^2}{m}\left(\chi_c^*(-\omega) - \chi_c(\omega)\right)\right) = \tilde{f}^z_{th}, \tag{44}$$

which brings us to usual cavity cooling result. Although not being optimal, we could place nanosphere to satisfy both $\sin(kx_0) = 1$ (mode node) and $\cos(kx_0) = 1$ (mode antinode) if we wish to cool both x and z directions. On the other side, we have already observed that z-motion is not orthogonal to cavity axis in our current setup, rather at angle $\sim 82°$. Due to this, we couple z-motion to cavity as well, however only with around 10^{-2} smaller rate than coupling x-motion. This would give us modest cooling rates, however enable us to have full three-dimensional cavity cooling of nanosphere motion.

6.1.3 *Phase noise*

Conclusion of our calculations is that optimal position for cavity cooling will be at a cavity node, where no light field at drive frequency is created. Moreover, this is the position where no phase noise will couple to cavity. Including phase noise in drive as $E_t\exp(-i(\omega t + \varphi(t)))$, we see there is no essential difference between phase $\varphi(t)$ and $kz(t)$. We have already shown that cavity amplitude $\hat{a}$ is not influenced by z-motion at cavity node ($\cos(kx_0) = 0$). Likewise, phase noise won't couple to amplitude if nanosphere is placed at this position.

6.1.4 *Cavity birefringence*

Induced by stress or by manufacturing imprecisions, any cavity will experience birefringence, i.e. resonant frequencies will depend on polarization. Furthermore, depending on stress and mirror symmetry, cavity polarization axes are rather a combination of vertical and horizontal polarization depending on birefringence angle θ: $V \to \sin\theta H + \cos\theta V$ and $H \to \cos\theta H - \sin\theta V$. Trapping laser will be vertically polarized in order to scatter into cavity, hence scattering will be split into both cavity polarizations. Both angle θ and frequency separation $\omega_c^1 - \omega_c^2$ are crucial to successful and strong cavity cooling. If angle $\theta \neq 0$, we have to be red detuned from both cavity modes, as cavity drive between ω_c^1 and ω_c^2 might lead to net heating of nanosphere motion (in the best case, worse cooling). Measurements of cavity birefringence will be presented in the experimental section.

6.2 Optomechanical cooperativity

We are ultimately interested in the optomechanical cooperativity one can reach in this approach. Assuming gas damping gives negligible heating, we concetrate on recoil heating from cavity and tweezer lasers (cite Quidant):

$$\Gamma_r^{tw} = \frac{4}{5}\frac{\omega_l}{\omega_0}\frac{I_0}{mc^2}\frac{k^4|\alpha|^2}{6\pi\varepsilon_0^2}, \tag{45}$$

where I_0 is intensity of an arbitrary laser at nanosphere position. We split cooperativity $C = \frac{4g_0^2 n_{phot}}{\kappa\Gamma_{rec}}$ by source of recoil heating:

$$\begin{aligned} C_{tw} &= 15\frac{U_0^2}{\left(\frac{\kappa}{2}\right)^2+\Delta^2}\frac{\mathcal{F}/\pi}{k^2 w_0^2} \text{ and} \\ C_{cav} &= \frac{240\mathcal{F}/\pi}{k^2 w_0^2}, \end{aligned} \tag{46}$$

where total cooperativity is given by $C = \frac{C_{tw}C_{cav}}{C_{cav}+C_{tw}}$. Already for modest cavity parameters which we have now ($\mathcal{F} = 70000$, $w_0 \approx 40\mu m$, $\kappa \approx 2\pi \times$ 200 kHz, $\Delta \approx 2\pi \times 150$ kHz and $U_0 \approx 2\pi \times 15$ kHz) we obtain $C \approx 2$, a significant improvement over current numbers.

7 EXPERIMENT

Our theoretical study was giving quite promising numbers, so we turned to defining experimental methods we need to implement in our experiment at the University of Vienna. These methods have already been realized at the host university, so this was an excellent opportunity for a knowledge transfer. Methods we are interested in investigating were:

7.1 Creation of cavity drive laser beam and external laser beam:

Right now, we use electro-optical modulators (EOMs) in order to create control laser cavity mode. We plan to combine this mode directly with trapping laser and drive nanosphere. However, this is not the optimal use as we would still have a significant part of laser light used only for trapping. We explored other possibilities in cooperation with group at the host university. The most promising strategy will be to lock the trapping laser to cavity mode with a constant frequency separation, hence using all of the trapping power for cavity cooling when needed. This will be implemented at the home university only in later stages of the experiment.

7.2 Laser frequency and power stabilization methods:

Currently, we use laser piezo to lock laser to cavity, in order to follow for any cavity drifts. We know from measurements of resonant frequencies that cavity drifts are smaller than $\lambda/2$. This laser will be modulated by free spectral range $\Delta\nu_{FSR} + \Delta$ and combined with trapping laser in order to achieve cavity cooling. Although not locked to any cavity resonance, created mode will be enough to demonstrate cavity cooling by coherent scattering. Further improvements will include locking a mode detuned to cavity resonance directly.

7.3 Cavity birefringence:

First step toward estimates of cooling rates in our new scheme is to determine orientation of cavity polarizations, which can be a linear combination of horizontal and vertical polarization. We set up a halfwave plate (HWP) in front of cavity in order to choose which of the two TEMoo modes (with equal longitudinal number) we drive. In the cavity transmission we set up another HWP and a polarizing beamsplitter (PBS), in which outputs we have two powermeters to detect polarization ratio of each cavity mode. We confirm that mode polarizations fall perfectly within horizontal/vertical polarizations. As cavity mirrors have been cut into thin strips to accommodate tweezer laser, we are not surprised to see that realized geometry is conforming cavity modes to this orientation. Scattered mode will drive vertically polarized cavity mode, while we can use horizontally polarized cavity mode to stabilize laser to it.

7.4 Exploring different cavity designs

Ultimately, strength of cavity colling and optomechanical cooperativity are defined by cavity geometry, i.e. its cavity mode volume $V_{cav} = \frac{w_0^2 \pi L}{4}$ as $g_0 \propto 1/V_{cav}$ and $C \propto 1/w_0^2$. Most stable configuration is a confocal cavity with length $L = RoC_1 = RoC_2$, where RoC_1 and RoC_2 are mirrors' radii of curvature. Cavity mode waist is simply $w_0 = \sqrt{\frac{L\lambda}{2\pi}}$ in this case. However, given radii of curvature, cavity with perpetually hold a mode for any cavity length such that $0 \leqslant \left(1 - \frac{L}{RoC_1}\right)\left(1 - \frac{L}{RoC_2}\right) \leqslant 1$. We explore multiple cavity configurations with main concerns being about stability, waist size and design time.

- **Concentric cavity.** In a case when $L = RoC_1 + RoC_2 - \delta L$ with $\delta L \to 0$, waist will quickly decrease. However, this cavity would be quite susceptible toward any translational or rotational drifts. Thus, one needs to invest significant considerations into a good, stable design. Experience from work of other groups tells us that design time measures in years. Minimum stable waist attained is $\sim 14\mu m$.

- **Microcavity.** In a case when $L \to 0$, two mirrors are almost touching. Besides the fact that any rotational movement would destroy mode as well, there is also a problem of fitting a tweezer trap in between cavity mirrors. Waists can be as small as in the case of concentric cavities.

- **"Quasi-confocal" cavity.** Made out of two different mirrors with $RoC_1 = 10$ mm as big as usual and one micromirror with $RoC_2 \approx 0.5\mu m$, it owes its name to stability which is seen only with confocal cavities. Stable cavity regions are for $RoC_1 < L < RoC_2$, with configuration with length $L = \frac{RoC_1 + RoC_2}{2}$ being stable over as big range as $\sim RoC_2$. Waist depends only on smaller RoC_2 and can be as small as $\sim 8\mu m$. These cavities are in use for the last couple of years at the host university, giving us a chance to see it in operation.

Of all cavity designs mentioned above, "quasi-confocal" cavity is the most promising. Knowledge obtained at the host university was immensely beneficial. We have obtained micromirrors to design cavities like this at the home university, which will be our plan in the following months. Combined with newly developed method of cavity cooling with coherent scattering, we will be able to reach unprecedentedly high cooperativity.

8 OUTCOME OF THE RESEARCH STAY

Following in steps of research done with atoms, we were poised to ponder if we could improve cooperativity by utilizing the external trapping beam in the current setup at the University of Vienna. For example, if the trapping beam is on resonance with an optical cavity, for certain position of nanosphere we could expect constructive or destructive interference of scattered photons, which has been described for atoms [27]. This so-called Purcell effect is an effective demonstration of cavity quantum electrodynamics (QED). However, we showed that in theory a detuned trapping laser mode can also constructively interfere scattered photons which pick up a quanta of nanosphere motional energy, hence conducting cooling. At yet another configuration of our setup, we could expect partial constructive interference of scattered photons, which could be used to extract nanosphere motional energy along two (or potentially three) axes, thus demonstrating more than one-dimensional cavity cooling of levitated nanospheres for the first time. This method doesn't have to be used alone; we intend to combine conventional cavity cooling and cooling by coherent scattering to boost cooperativity and show quantum control over nanosphere motion. Note that all our current setup (Figure 2) already allows for an external laser beam (trapping beam focused by an objective), which we need to slightly modify to test for coherent scattering.

So far, effect of coherent scattering and amplification of scattered light by a cavity (Purcell effect) has been shown solely on atoms in an optical cavity. I have concluded my research stay at the host university with a firm handle on the theory of coherent scattering, as well as a grasp on several new experimental techniques. I came up with a series of tests to do on-site, which will give us a definite view of method in question. A clear plan for a set of measurements at the University of Vienna has been devised, where we will focus on proving that an empty optical cavity can indeed be used for cavity cooling of a nanosphere. Furthermore, this experimental configuration will be continuously used in any further measurement as means to increase light-nanosphere interaction and come ever closer to room-temperature quantum experiments.

REFERENCES

[1] M. Aspelmeyer, T. J. Kippenberg, and F. Marquardt. Cavity Optomechanics. *ArXiv e-prints*, March 2013.

[2] O. Romero-Isart, M. L. Juan, R. Quidant, and J. I. Cirac. Toward quantum superposition of living organisms. *New Journal of Physics*, 12(3):033015, March 2010.

[3] D. E. Chang, C. A. Regal, S. B. Papp, D. J. Wilson, J. Ye, O. Painter, H. J. Kimble, and P. Zoller. Cavity opto-mechanics using an optically levitated nanosphere. *Proceedings of the National Academy of Science*, 107:1005–1010, January 2010.

[4] P. F. Barker. Doppler Cooling a Microsphere. *Physical Review Letters*, 105(7):073002, August 2010.

[5] A. A. Geraci, S. B. Papp, and J. Kitching. Short-Range Force Detection Using Optically Cooled Levitated Microspheres. *Physical Review Letters*, 105(10):101101, September 2010.

[6] O. Romero-Isart, A. C. Pflanzer, F. Blaser, R. Kaltenbaek, N. Kiesel, M. Aspelmeyer, and J. I. Cirac. Large quantum superpositions and interference of massive nanometer-sized objects. *Phys. Rev. Lett.*, 107:020405, Jul 2011.

[7] S. G. Hofer, D. V. Vasilyev, M. Aspelmeyer, and K. Hammerer. Time-Continuous Bell Measurements. *Physical Review Letters*, 111(17):170404, October 2013.

[8] N. Kiesel, F. Blaser, U. Delić, D. Grass, R. Kaltenbaek, and M. Aspelmeyer. Cavity cooling of an optically levitated nanoparticle. *ArXiv e-prints*, April 2013.

[9] J. Millen, P. Z. G. Fonseca, T. Mavrogordatos, T. S. Monteiro, and P. F. Barker. Cavity Cooling a Single Charged Levitated Nanosphere. *Physical Review Letters*, 114(12):123602, March 2015.

[10] P. Z. G. Fonseca, E. B. Aranas, J. Millen, T. S. Monteiro, and P. F. Barker. Nonlinear Dynamics and Strong Cavity Cooling of Levitated Nanoparticles. *Physical Review Letters*, 117(17):173602, October 2016.

[11] P. Asenbaum, S. Kuhn, S. Nimmrichter, U. Sezer, and M. Arndt. Cavity cooling of free silicon nanoparticles in high vacuum. *Nature Communications*, 4:2743, November 2013.

[12] V. Jain, J. Gieseler, C. Moritz, C. Dellago, R. Quidant, and L. Novotny. Direct Measurement of Photon Recoil from a Levitated Nanoparticle. *Physical Review Letters*, 116(24):243601, June 2016.

[13] J. Gieseler, B. Deutsch, R. Quidant, and L. Novotny. Subkelvin Parametric Feedback Cooling of a Laser-Trapped Nanoparticle. *Physical Review Letters*, 109(10):103603, September 2012.

[14] V. Vuletić, H. W. Chan, and A. T. Black. Three-dimensional cavity Doppler cooling and cavity sideband cooling by coherent scattering. *Physical Review A*, 64(3):033405, September 2001.

[15] E. M. Purcell, H. C. Torrey, and R. V. Pound. Resonance Absorption by Nuclear Magnetic Moments in a Solid. *Physical Review*, 69:37–38, January 1946.

[16] H. W. Chan, A. T. Black, and V. Vuletić. Observation of Collective-Emission-Induced Cooling of Atoms in an Optical Cavity. *Physical Review Letters*, 90(6):063003, February 2003.

[17] M. Hosseini, Y. Duan, K. M. Beck, Y.-T. Chen, and V. Vuletić. Cavity Cooling of Many Atoms. *Physical Review Letters*, 118(18):183601, May 2017.

[18] H. Tanji-Suzuki, I. D. Leroux, M. H. Schleier-Smith, M. Cetina, A. T. Grier, J. Simon, and V. Vuletić. Interaction between Atomic Ensembles and Optical Resonators. *Advances in Atomic Molecular and Optical Physics*, 60:201–237, 2011.

[19] M. Bienert and G. Morigi. Cooling the motion of a trapped atom with a cavity field. *Physical Review A*, 86(5):053402, November 2012.

[20] S. Nimmrichter, K. Hammerer, P. Asenbaum, H. Ritsch, and M. Arndt. Master equation for the motion of a polarizable particle in a multimode cavity. *New Journal of Physics*, 12(8):083003, August 2010.

[21] O. Romero-Isart, A. C. Pflanzer, M. L. Juan, R. Quidant, N. Kiesel, M. Aspelmeyer, and J. I. Cirac. Optically levitating dielectrics in the quantum regime: Theory and protocols. *Physical Review A*, 83(1):013803, January 2011.

[22] A. C. Pflanzer, O. Romero-Isart, and J. I. Cirac. Master-equation approach to optomechanics with arbitrary dielectrics. *Physical Review A*, 86(1):013802, July 2012.

[23] E. M. Purcell, H. C. Torrey, and R. V. Pound. Resonance Absorption by Nuclear Magnetic Moments in a Solid. *Physical Review*, 69:37–38, January 1946.

[24] A. A. Clerk, M. H. Devoret, S. M. Girvin, Florian Marquardt, and R. J. Schoelkopf. Introduction to quantum noise, measurement, and amplification. *Rev. Mod. Phys.*, 82:1155–1208, Apr 2010.

[25] M. Hosseini, Y. Duan, K. M. Beck, Y.-T. Chen, and V. Vuletić. Cavity Cooling of Many Atoms. *Physical Review Letters*, 118(18):183601, May 2017.

[26] C. Genes, D. Vitali, P. Tombesi, S. Gigan, and M. Aspelmeyer. Ground-state cooling of a micromechanical oscillator: Comparing cold damping and cavity-assisted cooling schemes. *Phys. Rev. A*, 77(3):033804, March 2008.

[27] M. Motsch, M. Zeppenfeld, P. W. H. Pinkse, and G. Rempe. Cavity-enhanced Rayleigh scattering. *New Journal of Physics*, 12(6):063022, June 2010.